J. Membrane Biol. 131, 11–22 (1993)

The Journal of
Membrane Biology

Pore Formation by the Sea Anemone Cytolysin Equinatoxin II in Red Blood Cells and Model Lipid Membranes

Giovanna Belmonte†, Cecilia Pederzolli†‡, Peter Maček§, and Gianfranco Menestrina†‖
†Dipartimento di Fisica, Universitá di Trento, I-38050 Povo (TN), Italy, ‡Istituto per la Ricerca Scientifica e Tecnologica, I-38050 Povo (TN), Italy, §Department of Biology, Biotechnical Faculty, University of Ljubljana, SLO-61000 Ljubljana, Slovenia, and ‖CNR Centro di Fisica degli Stati Aggregati I-38050 Povo (TN), Italy

Summary. The interaction of *Actinia equina* equinatoxin II (EqT-II) with human red blood cells (HRBC) and with model lipid membranes was studied. It was found that HRBC hemolysis by EqT-II is the result of a colloid-osmotic shock caused by the opening of toxin-induced ionic pores. In fact, hemolysis can be prevented by osmotic protectants of adequate size. The functional radius of the lesion was estimated to be about 1.1 nm. EqT-II increased also the permeability of calcein-loaded lipid vesicles comprised of different phospholipids. The rate of permeabilization rised when sphingomyelin was introduced into the vesicles, but it was also a function of the pH of the medium, optimum activity being between pH 8 and 9; at pH 10 the toxin became markedly less potent. From the dose-dependence of the permeabilization it was inferred that EqT-II increases membrane permeability by forming oligomeric channels comprising several copies of the cytolysin monomer. The existence of such oligomers was directly demonstrated by chemical cross-linking. Addition of EqT-II to one side of a planar lipid membrane (PLM) increases the conductivity of the film in discrete steps of defined amplitude indicating the formation of cation-selective channels. The conductance of the channel is consistent with the estimated size of the lesion formed in HRBC. High pH and sphingomyelin promoted the interaction even in this system. Chemical modification of lysine residues or carboxyl groups of this protein changed the conductance, the ion selectivity and the current-voltage characteristic of the pore, suggesting that both these groups were present in its lumen.

Key Words equinatoxin II (*Actinia equina*) · membrane damage · hemolysis · pore formation · size determination · ion selectivity · chemical modification

Introduction

Sea anemones produce polypeptide and protein toxins that are collected in specialized cells, the nematocysts. According to their function, these toxins can be separated into neurotoxins, acting on the excitable sodium channel [23, 42] and cytotoxins (or cytolysins) with a broader spectrum of action [23]. Potent cytolysins have been extracted from the venom of at least sixteen species of sea anemones [4, 18, 23], of which they constitute the most active part. They have similar properties: they are highly basic protein toxins, with pI between 8 and 12, and are made up of a single polypeptide chain of molecular weight between 10 and 20 kD. Many of them have been isolated and a few have been sequenced [23]. They cause erythrocyte and platelet lysis at very low concentrations (nanomoles) and are generally inhibited by sphingomyelin. There is no definitive understanding of the mechanism of action of these toxins. Some of them cause an increase in the permeability of cells and model lipid membranes [38, 55, 58] to small ions and solutes, probably by the formation of discrete pores, but whether this is the necessary and sufficient cause of their many physiological activities is still debated.

One such cytolysin, equinatoxin II from *A. equina* was isolated recently and purified to homogeneity [33]. It is hemolytic [32], cytotoxic [1], cardiotoxic [20,29] and causes platelet aggregation [50] and lung damage [26]. It was proposed that at least part of these effects can be ascribed to its ability to form ion channels [58]. We have now studied the interaction of this toxin with human red blood cells and with artificial lipid membranes (unilamellar vesicles and planar bilayers) to better characterize the properties of the pore it forms.

Abbreviations

EqT-II: *Actinia equina* equinatoxin II; SM: sphingomyelin; PC: phosphatidylcholine; PE: phosphatidylethanolamine; POPC: palmitoyl-oleoyl-phosphatidylcholine; SUV: small unilamellar vesicles; HRBC: human red blood cells; PLM: planar lipid membranes; TLC: thin layer chromatography; SDS: sodium dodecyl sulfate; LDS: lithium dodecyl sulfate; Tween-20: polyoxyeth-

Table 1. Solutions and compositions (in mmol/liter)

Solution	Na^+	K^+	Cl^-	$H_2PO_4^-$	$Citrate^{3-}$	EDTA	Dextrose	Buffer	pH
ACD	225	—	—	—	156	—	111	—	4.6
PBS	250	—	150	100	—	—	—	—	7.4
5P8	5	—	—	5	—	—	—	—	8.0
Saline	145	—	145	—	—	—	—	—	6.7
A	140	—	140	—	—	1	—	10[a]	8.0
B	—	100	100	—	—	—	—	10[b]	10 ÷ 4
C	100	—	100	—	—	—	—	10[b]	10 ÷ 4

[a] Tris
[b] The following buffers were used for the pH range indicated in parentheses: Caps (pH 10 ÷ 8), HEPES (pH 8 ÷ 6), citrate (pH 5 ÷ 4).

ylene sorbitan monolaurate; Brij-35: polyoxyethylene(23)lauryl ether; Triton X-100: octylphenoxy polyethoxy ethanol; Lubrol-PX: polyethylenglycol(9)dodecyl ether; PLP: pyridoxal-5'-phosphate; EDC: 1-ethyl-3-(3'-dimethylaminopropyl)-carbodiimide; DMS: dimethyl suberimidate; PEG: polyethyleneglycol.

Materials and Methods

Chemicals

Toxins

A. equina equinatoxin II, called EqT-II, was purified and assayed as described [33]. Chemical modification of the lysine residues by PLP was performed according to [41] exactly as described earlier [53]. The number of moles of lysine residues modified per mol of toxin was determined spectrophotometrically [43]. The carboxyl groups of aspartic or glutamic acid residues were modified by carbodiimide (EDC) according to [11] as already described [53, 54]. Undesired modification of tyrosine residues was reversed by exposure to hydroxylamine [53]. The extent of carboxyl groups modification was determined by amino acid analysis as described [53].

Others

Sphingomyelin from bovine brain, egg phosphatidylcholine and bacterial phosphatidylethanolamine were purchased from Calbiochem; palmitoyl-oleoyl-phosphatidylcholine came from Avanti Polar Lipids. All lipids were more than 99% pure by TLC. The buffer solutions used are listed in Table 1. The following sugars were used as osmotic protectants: sucrose, raffinose, maltohexaose and maltoheptaose by Sigma stachiose and maltopentaose by Janssen, dextrose, dextran 1600 and 6000, PEG 1000, 1500, 2000, 3000 and 4000 all purchased from Fluka (the numbers represent their average molecular weight). Hydroxylamine was from Janssen Chimica; calcein, dimethyl suberimidate and Sephadex-G50 were obtained through Sigma Chemical; SDS, Lubrol-PX, Tween-20 and Brij-35 were from Pierce Chemical; LDS from Fluka; Triton X-100 from Merck.

Assays

Kinetics of Hemolysis

HRBC were prepared from freshly collected venous blood (supplemented with 1% buffer ACD) and washed thrice in saline buffer. The time course of red blood cell lysis induced by EqT-II (typically 50 ng/ml), was followed spectrophotometrically at 700 nm with a Perkin-Elmer 551 spectrophotometer in a 1-cm cuvette at 25°C as described previously [32]. HRBC were suspended at a concentration of 0.05% in Buffer A (either pure or supplemented with 30 mM of different sugars as specified in the text) and continuously stirred. Initially $A_{700\,nm}$ was about 0.5.

Permeabilization of Lipid Vesicles

EqT-II permeabilization of small unilamellar vesicles was assayed as described earlier [12, 34, 44]. Briefly, aliquots of vesicles sonicated in the presence of 80 mM calcein and washed with Sephadex-G50 were introduced into a 1-cm semimicro quartz cuvette containing 1 ml of Buffer C at 24 or 30°C. The final lipid concentration was typically 2–4 μg/ml and the solution was continuously stirred. After mixing with toxin, the release of calcein from the vesicles produced an increase in the fluorescence F emitted at 520 nm (excitation at 494 nm), due to the dequenching of the dye into the external medium. Maximum release, yielding the fluorescence F_{max}, was determined by addition of 0.4 mM Triton X-100. The extent of permeabilization, P, was calculated as percentage of the maximum release obtained with Triton X100, as follows:

$$P(\%) = (F_{fin} - F_{in})/(F_{max} - F_{in}) \cdot 100 \quad (1)$$

where F_{in} and F_{fin} represent the initial and final value of fluorescence before and after toxin addition, respectively.

The rate of permeabilization, k, was determined as the initial slope of each curve divided by the maximum release, i.e.:

$$k = dF/dT|_{in}/(F_{max} - F_{in}) \quad (2)$$

Spontaneous release of calcein was negligible under these conditions.

Channel Formation in Planar Lipid Bilayers

Planar lipid membranes (PLM) were prepared as described earlier [2, 7] by apposing two lipid monolayers on a 0.2 mm hole in a thin Teflon septum separating two buffered salt solutions. The monolayers were spread using the mixture POPC : PE 4 : 1, dissolved at 10 mg/ml in *n*-hexane.

EqT-II was added to the *cis* compartment of a preformed stable bilayer and the current flowing through the membrane, under voltage-clamp conditions, was passed through an *I-V* converter (a virtual grounded AD515K operational amplifier). *Cis* compartment was connected to the virtual ground and voltage signs refer to it; current is defined positive when cations flow into this compartment. Baseline conductance of the membranes did not exceed 50 pS. Ag-AgCl electrodes were used. Bathing solutions, 4 ml of Buffer A on each side, were kept at room temperature.

Chemical Cross-Linking

Cross-linking with DMS (dimethylsuberimidate) was carried out according to Davies and Stark [8]. DMS was dissolved in buffer PBS, pH 8.5, just before use. The cross-linking reaction was initiated by adding small aliquots of DMS to either free toxin or toxin incubated with SUV. Incubation was performed as follows: 50 μl of sonicated vesicles comprised of SM : PC (4 : 1 molar ratio) and suspended at a lipid concentration of 2 mg/ml in buffer PBS at pH 9.0 were mixed with an equal amount of the same buffer plus EqT-II (usually 4 mg/ml); the mixture was incubated at 37°C for 30 min. The toxin to DMS ratio was varied but a value of 4 : 1 (in weight) was found to be optimal. The reaction was allowed to run at room temperature for different times (as specified in the text). Finally it was stopped by addition of 10 mM hydroxylamine, and the cross-linked samples were analyzed by polyacrylamide gel electrophoresis.

Polyacrylamide Gel Electrophoresis

Denaturing gel electrophoresis was performed according to Laemmli [25] except that the run was at 4°C in a buffer containing 0.3% LDS. We used precast gradient minigels (Pharmacia, Uppsala, Sweden) with densities ranging either 8–25% or 10–15% (as specified in the text). A semi-automatic unit, Phast-System by Pharmacia, was employed. Gels were stained with Coomassie brilliant blue or with silver stain and the amount of protein was quantitated by bidimensional densitometry using a PhastImage densitometer (Pharmacia) with a band-pass filter at 613 nm, for Coomassie-stained gels, or at 546 nm, for silver-stained gels. The relative toxin concentration was obtained as the optical volume of the corresponding band measured in mOD · mm^2. All protein samples were made 1.6% in LDS before running on the gel; in the case of toxin that had been incubated with SUV, small amounts of different non-ionic detergents were also included to improve lipid solubilization and avoid streaking of the lanes. We tried Triton X-100, Tween-20, Brij-35 and Lubrol-PX and found that the last gave the best results.

In native-PAGE proteins were separated in the absence of dodecylsulfate at pH 8.8 and migrated according to their intrinsic net charge [21]. Minigels with linear gradients of 8% to 25% were used and the run was performed at 10°C.

Results

Hemolysis of red blood cells exposed to equinatoxin II may result from a colloid-osmotic shock caused by the opening of ionic pores formed by the toxin itself [58]. To test this we decided to investigate whether the addition of osmotic protectants into the external solution could prevent hemolysis, as is the case for *Staphylococcus aureus* α-toxin [5] and *Pseudomonas aeruginosa* cytotoxin [56]. We measured spectrophotometrically the kinetics of hemolysis of HRBC exposed to this cytolysin in the presence of sugars of increasing size (Fig. 1*A*). Indeed, the addition of osmoticants can considerably prolong the lag time before the onset of hemolysis and reduce its rate. The extent of both these effects depends on the size of the molecule. In the colloid-osmotic hypothesis this delay is due to the time necessary for the osmoticant to diffuse inside the cell through the toxin-induced lesions. As an estimate of this time we used $t_{1/2} - t^{\circ}_{1/2}$, (where $t_{1/2}$ and $t^{\circ}_{1/2}$ are the time to reach 50% of hemolysis with or without osmotic protectants, respectively). Accordingly $1/(t_{1/2} - t^{\circ}_{1/2})$ gives an estimate of the rate of solute diffusion through the pore, which we used to build a so-called Renkin plot [16, 45] (Fig. 1*B*) reporting the relative permeability of the molecule *vs.* its size. Such a plot allows estimation of the functional radius of the lesion in about 1.1–1.2 nm. Molecules of a radius larger than 1.0 (i.e., Peg 1,000, 1,500, 2,000, 3,000, 4,000 and dextran 6,000) prevented hemolysis, suggesting they were impermeant.

Having shown that toxin-induced RBC lysis results from the formation of toxin channels into the cell membrane we were prompted to investigate whether the toxin can form pores also in model lipid bilayers, as shown for many other cytolytic toxins [35, 36]. We observed that addition of EqT-II to a solution containing small unilamellar vesicles loaded with calcein (at a self-quenching concentration) indeed promoted the release of the dye, as indicated by an increase of the fluorescence (Fig. 2). The time course of the kinetics of interaction of the toxin with the vesicles and its dependence on their lipid composition (Fig. 2*A*) and on the pH of the bath (Fig. 2*B*) could thus be determined. From such traces the rate and the extent of permeabilization were calculated as described in Materials and Methods (Fig. 3*A* and *B*, respectively). We observed that both these variables increased by introducing sphingomyelin into the vesicles. In fact, the percentage of release was at most 5% in vesicles comprised of pure PC, and the rate constant was at least two orders of magnitude smaller than with sphingomyelin-containing vesicles. Even small amounts of sphingomyelin (11%) were sufficient to render the vesicles quite

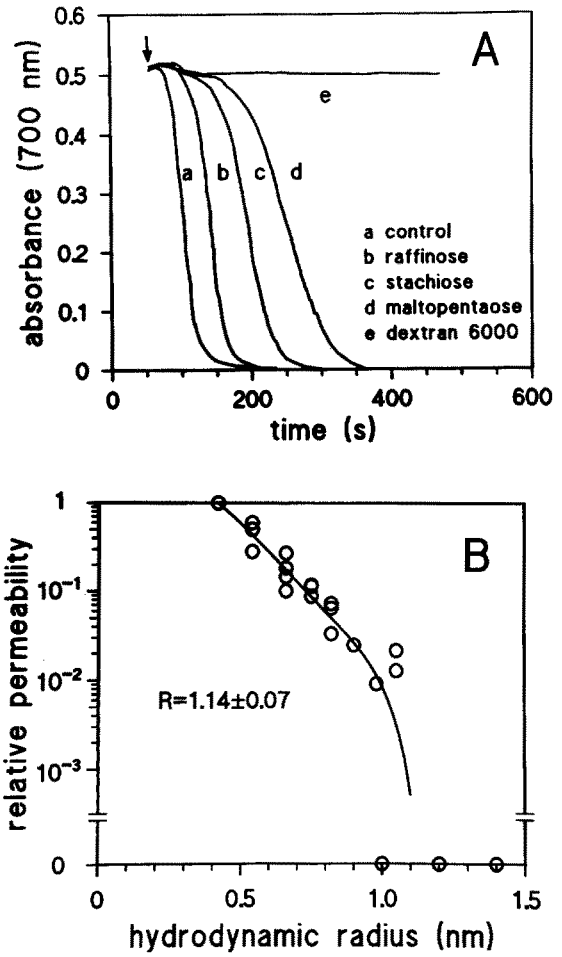

Fig. 1. EqT-II induced lysis of human erythrocytes in the presence of osmotic protectants. (*A*) HRBC suspended in Buffer A (either pure or supplemented with 30 mM of the indicated sugars) at a concentration of 0.05% and continuously stirred, were exposed to 50 ng/ml of EqT-II (arrow). The decrease of $A_{700\,nm}$ indicates hemolysis. We obtained $t_{1/2}$ (i.e., the time necessary to reach 50% of hemolysis) from these kinetics. As an indicative parameter of the time necessary for the sugar molecules to enter the cells through the toxin-induced lesions we used $t_{1/2} - t^0_{1/2}$, where $t^0_{1/2}$ is the time to 50% lysis without osmotic protectants. Accordingly the rate of solute diffusion through the pore is proportional to $1/(t_{1/2} - t^0_{1/2})$. Dextran 6,000 completely prevented hemolysis for several hours. (*B*) Renkin plot [16] reporting the relative diffusion rate of the osmoticant molecule (as compared to dextrose) *vs.* its size. Hydrated radii used were taken from [24, 49]. Solid line is a best fit according to the Renkin equation [45], yielding a functional radius of the lesion of 1.14 ± 0.07 nm. PEG 1,000, 1,500, 2,000, 3,000, 4,000 and dextran 6,000 (with radius 1.0, 1.2, 1.4, 1.7, 2.0 and 1.9 nm, respectively) were all fully protective. Dextran 1,500 (radius 1.05 nm) had a higher-than-expected permeability, which might be due to an elongated shape, and was not used to estimate the best-fit radius.

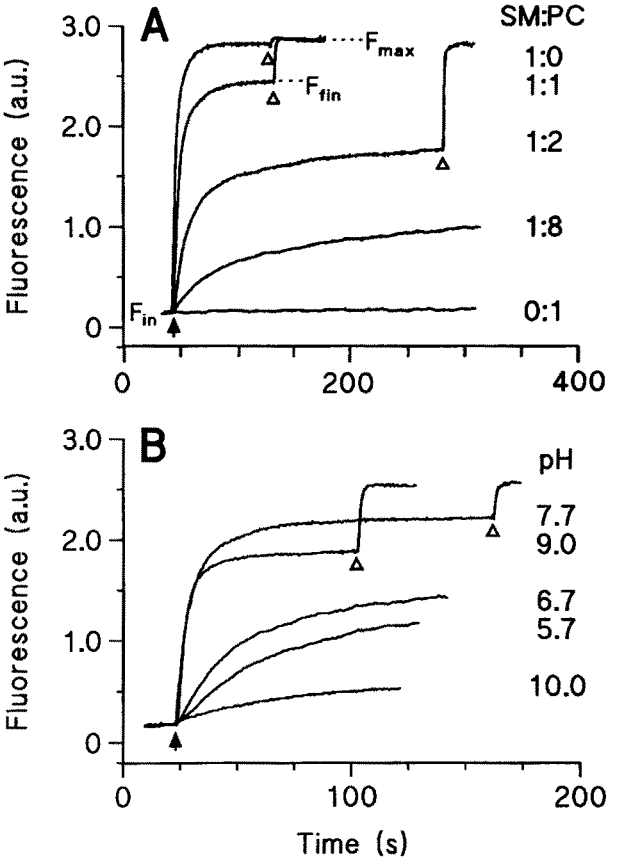

Fig. 2. Permeabilizing activity of EqT-II on SUV measured by the release of calcein. (*A*) Fluorescence, $F(t)$ measured in arbitrary units, increases after the addition of 2 μg/ml EqT-II, indicated by an arrow, to a solution containing SUV loaded with calcein (2 μg/ml of lipid). $F(t)$ eventually reaches a steady value indicated as F_{fin}. The fluorescence increase indicates that the dye is released from the vesicles in which it was entrapped at a self-quenching concentration. Maximal release, F_{max}, was obtained by the addition of 0.4 mM Triton X-100, indicated by open arrowheads. SUV of different lipid compositions were used: pure SM, pure PC and three SM/PC mixtures. For the sake of comparison in this figure the traces were scaled so as to give the same F_{max} in all cases. Other experimental conditions are: external solution Buffer C, pH 7.7. Rate and extent of permeabilization were calculated from the initial slope and from the amplitude of these curves as indicated in the text. (*B*) Same as in *A*, but the effects of pH on EqT-II permeabilization of SUV comprised of an equimolar SM : PC mixture, were investigated. Optimum activity is observed around pH 8 to 9.

sensitive to the toxin; however, for maximum effect, at least 50% was required.

As far as the pH is concerned, we noticed that in general the activity of EqT-II increased by increasing the pH of the solution. Optimum pH was between pH 8 and pH 9; at pH 10 the toxin became less potent, which might be due to a decrease in its electrical charge or to a conformational change. This pH dependence was exactly the same observed for the hemolysis of red blood cells [32], suggesting that the events leading to vesicle and erythrocyte permeabilization were in fact the same.

The dependence of the permeabilizing effect on

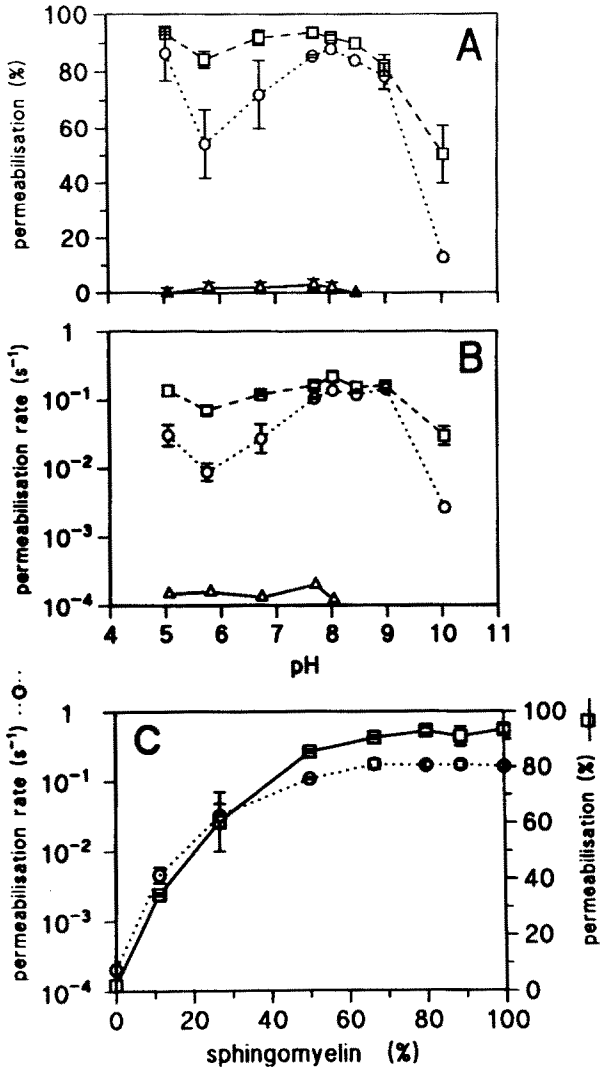

Fig. 3. Extent and rate of permeabilization of SUV of different composition as a function of pH. (*A*) Percentage of release, obtained as shown in Fig. 2, for vesicles comprised of different lipids. Symbols used (here and in panel *B*) are: SM, squares; SM/PC (1 : 1 mixture), circles; PC, triangles. (*B*) Rate of permeabilization calculated from the initial slope of release curves as those in Fig. 2. (*C*) Titration of the potentiating effect of sphingomyelin. Different SM to PC ratios were used to prepare the vesicles and the rate and extent of permeabilization by EqT-II at pH 7.7 were measured (left and right ordinate, respectively). Other experimental conditions (common to all panels): external solution Buffer C, toxin and lipid concentrations 2 μg/ml, 30°C; mean ± SD of three to four experiments are reported.

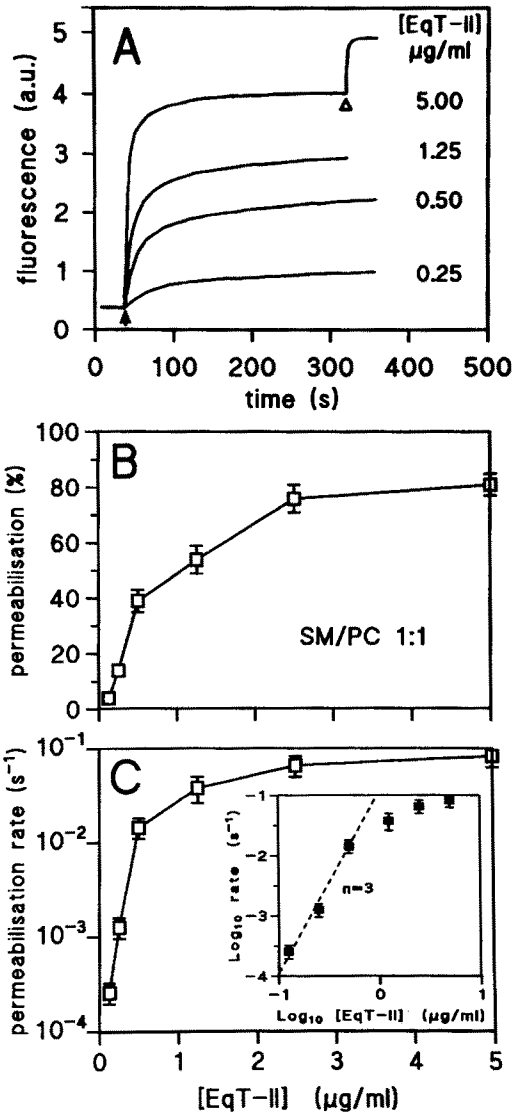

Fig. 4. Dose dependence of the EqT-II-induced SUV permeabilization. (*A*) Time course of calcein release from SM/PC vesicles (1 : 1 mixture) after addition (at the arrow) of different amounts of EqT-II (as indicated). Maximal release was obtained by the addition of 0.4 mM Triton X-100, indicated by an open arrowhead, and was the same for all SUV compositions. SUV were suspended in Buffer A, pH 8.0, at a lipid concentration of 2.5 μg/ml, 24°C. (*B*) Percentage of release *vs.* the concentration of added toxin; mean ± SD of three to four determinations are reported. (*C*) Rate of permeabilization *vs.* the concentration of added toxin. In the inset a double logarithmic plot of the dose-dependence curve is reported. Dashed line is a least-squares fit to the first part of the curve yielding a power dependence coefficient $n \simeq 3$. Error bars as in *B*.

the toxin dose was studied using sensitive vesicles (composed of an equimolar mixture of SM and PC) at pH 8 (Fig. 4). As expected, both the rate and the extent of calcein release increase with the toxin concentration (Fig. 4*A*). A plot of the percentage of release *vs.* toxin dose indicates that saturation occurs at a concentration of about 2.5 μg/ml (Fig. 4*B*), which is considerably larger than that for HRBC. However, a detectable effect was already present at a concentration of 0.125 μg/ml, i.e., about 6 nM. A double logarithmic plot (Fig. 4*C*) of the initial rate of release *vs.* toxin dose showed again saturation

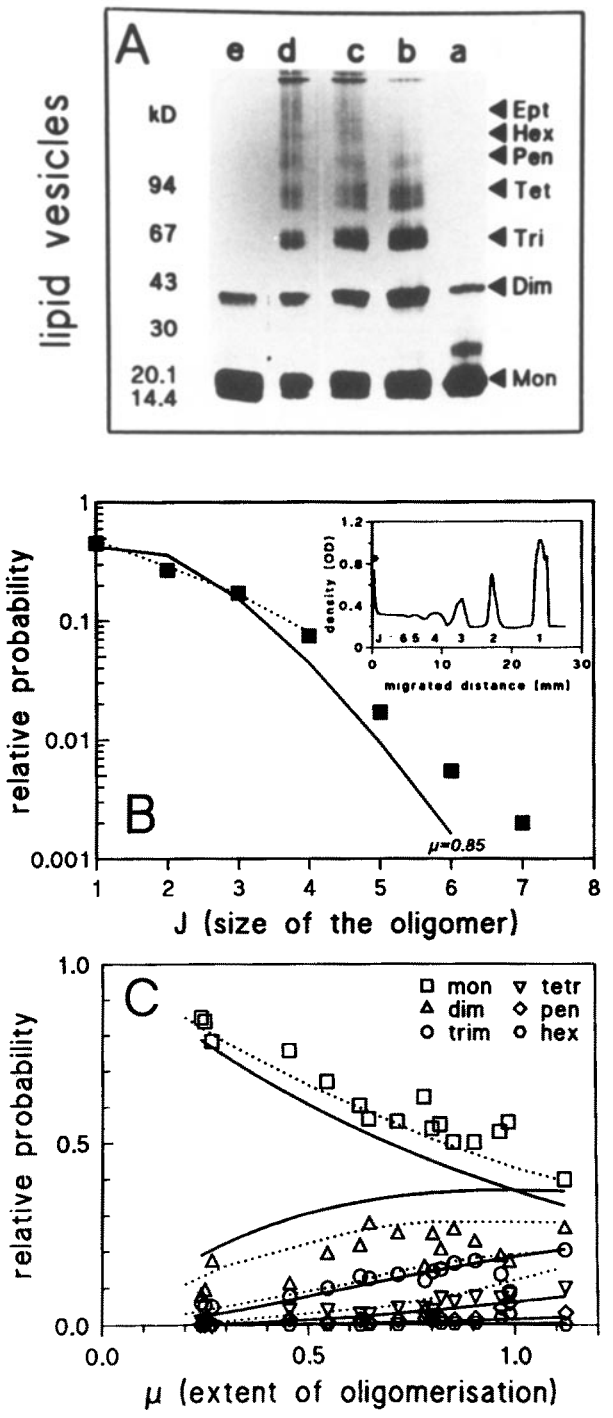

Fig. 5. Chemical cross-linking of free and membrane-bound EqT-II. (*A*) EqT-II oligomer formation on SUV comprised of SM : PC (4 : 1 molar ratio) evidentiated by polyacrylamide gel electrophoresis. Cross-linking with DMS was carried out in buffer PBS at pH 9.0, as described in Materials and Methods. Lane *a:* toxin incubated with SUV but not treated with DMS. Lane *b, c, d:* toxin incubated with SUV and treated with DMS for 1, 2, and 3 hr, respectively (the reaction was stopped by 8 mM hydroxylamine). Lane *e:* toxin treated with DMS for 3 hr but without previous incubation with SUV. The position of standard proteins of known molecular weight is shown on the left, full arrow-heads on the right extrapolate the average molecular weight of toxin oligomers. Experimental conditions: lipid concentration 0.77 mg/ml, toxin concentration 1.5 mg/ml, DMS 0.38 mg/ml, polyacrylamide gradient 10–15%, Lubrol-PX 0.06 mg/ml, LDS 1.6%, silver staining. (*B*) Densitometry of the LDS-PAGE (the example in the inset shows a volumogram of lane *c* of panel *A*) allows the position and the relative protein content of each band to be calculated independently. Bands are labeled with the index *j*, which gives the number of cross-linked toxin monomers present in the band. Density is given in absorption units. An asterisk marks the end of the stacking gel. The relative probability of each oligomer, called P_j, after 1 hr cross-linking, is represented by full squares in a half logarithmic plot. The solid line is the prediction of a random collisional model [9] that makes use of the index μ (calculated as $\mu = \Sigma_j(j-1)P_j$) to estimate the overall degree of cross-linking. The value of μ was 0.85 for this experiment. Dotted line is the theoretical prediction for a preexisting tetramer (derived from [9]). (*C*) Relative probability of each oligomer as a function of the overall degree of cross-linking μ. μ was varied by changing the concentrations of EqT-II and DMS, and the temperature and duration of the cross-linking reaction. Each set of symbols on a vertical line comes from the volumogram of a different lane. The solid lines are the predictions of the random collisional model, whereas the dotted lines are the predictions for a preexisting tetramer [9] and fit better.

(starting at a concentration of about 3μg/ml), but, intriguingly, it indicated also that the slope of the dose response has a value much larger than one in the early phase. This suggests that permeabilization may be the result of the assembly of an oligomeric toxin lesion on the vesicles, as observed with *S. aureus* α-toxin [12–14] and *Aeromonas hydrophila* aerolysin [15, 17].

However, in contrast to α-toxin and aerolysin (whose oligomers are stable in SDS [12, 17, 44], EqT-II failed to show stable aggregates when permeabilized vesicles were detergent-solubilized and electrophoresed in the presence of either SDS or LDS. Since this could be due to an instability of the complex in the presence of detergents, we decided to try to cross-link the aggregate formed on the membrane surface. This was done using the homobifunctional cross-linking agent DMS which has a chain length of 11 Å. Figure 5*A* shows that incubation of toxin-treated vesicles with DMS leads to the stabilization of oligomeric toxin structures containing various numbers of monomers (up to seven). Although pure toxin shows a certain amount of dimeric form even in buffer solution, no aggregate of size larger than two was observed (either with or without DMS) in the absence of membranes. This indicates that the formation of large oligomers was limited to the membrane bound form of EqT-II. The percentage of

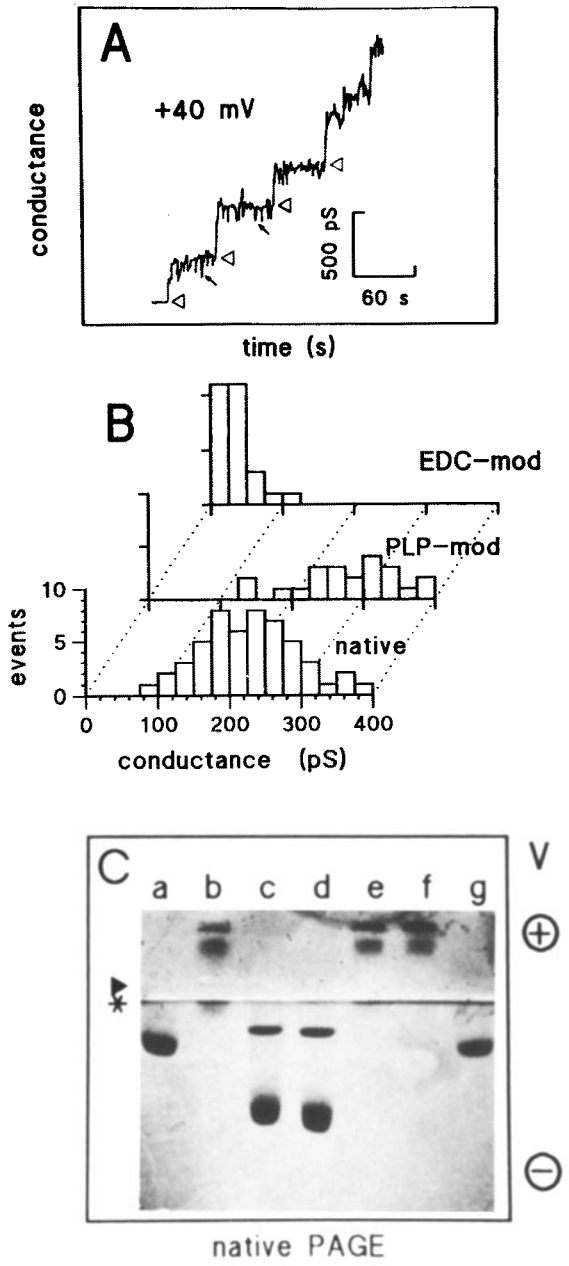

Fig. 6. (*A*) Addition of EqT-II to one side of a PLM resulted in the opening of ionic channels which increased the conductivity of the film in discrete steps of defined amplitude, indicated by open arrowheads. Open channels fluctuate between at least two different conductance levels (examples indicated by small arrows). A current amplitude for the fully open channel can be evaluated. Experimental conditions: toxin concentration 0.25 μg/ml, applied voltage +40 mV, Buffer B, pH 8.0. (*B*) Histograms showing the number of events with a given conductance observed in different experiments run with either native toxin or PLP-modified or EDC-modified samples. Experimental conditions as in *A*. (*C*) Effect of PLP- or EDC-modification on the electrical charge of EqT-II as determined by native-PAGE at pH 8.8. Lanes *a* and *g*: native toxin. Lanes *b*, *e*, *f*: PLP-modified toxin (3.8, 3.4, 4.6 lys residues modified per monomer, respectively). Lanes *c*, *d*: EDC-modified toxin. An arrowhead indicates the position at which the samples were applied, whereas an asterisk marks the end of the stacking gel, the polarity of the applied voltage is indicated by + and −. At this pH, native toxin is slightly positively charged. EDC-modified toxin becomes more positive and is further displaced toward the cathode, whereas PLP-modified toxin becomes negatively charged and migrates towards the anode.

large oligomers increased by prolonging the reaction with DMS (Fig. 5), but did not change increasing the toxin-SUV incubation time (*not shown*). This suggests that the SUV-toxin reaction goes to equilibrium very quickly as indicated also by the fast kinetics of permeabilization (Fig. 4*A*).

EqT-II Forms Ionic Channels in Planar Lipid Bilayers

Vesicle permeabilization most probably results from the formation of toxin channels into the lipid bilayer. In fact addition of EqT-II to one side of a voltage-clamped planar lipid membrane (PLM) increased the conductivity of the film in discrete steps of large amplitude (Fig. 6*A*) implicating the formation of pores. High pH and sphingomyelin promoted the interaction even in this system (*not shown*). Opening of one pore was usually followed by fluctuations of smaller size. Together with the fact that the distribution of channel amplitude observed was rather broad (Fig. 6*B*), this suggested that, also in the case of PLM, ionic channels may result from the assembly of heterogeneous toxin aggregates.

PLM are probably the best substrate to study a number of channel features such as conductance, selectivity and rectification [35, 36]. We took advantage of this to investigate the electrical properties of pores formed either by native toxin or by two chemically-modified species. In one case 3.4 mol of lysine residues per mol of toxin were modified by PLP. This reagent covalently replaces the positive charge of the lysyl amino group with a negative charge. As a result the toxin became less positively charged as confirmed by an electrophoresis performed under native conditions (Fig. 6*C*). In the other case, about 9 mol of carboxyl groups (aspartic or glutamic acid residues) per mol of toxin were modified by carbodiimide (EDC), which covalently replaces the negatively charged oxygen with an uncharged group. As a result, this time the toxin became more positively charged, as confirmed by the native gel electrophoresis (Fig. 6*C*). Both PLP- and EDC-modified toxin were still fully hemolytic, although the rate of hemolysis was slower for EDC-modified toxin as reported previously [53].

A comparison of the histograms relating the

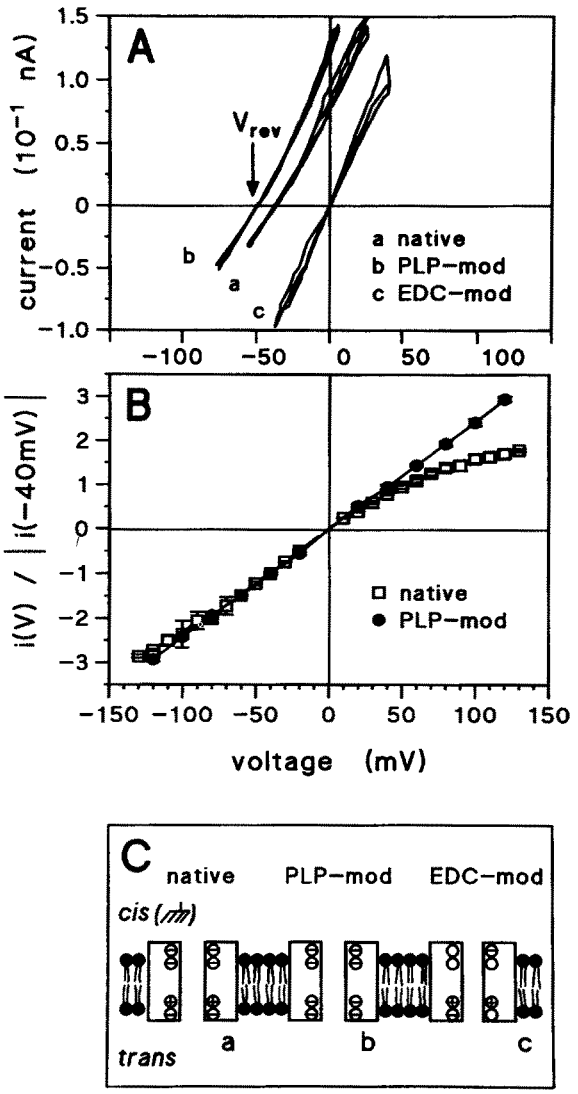

Fig. 7. Selectivity and current-voltage characteristic of native and chemically modified EqT-II pores. (*A*) Current-voltage curves obtained applying a slowly changing triangular wave of voltage to membranes containing a population of many channels (as observed several minutes after the addition of the protein). The membranes separated two asymmetrical solutions containing 50 mM NaCl on the *cis* side and 500 mM NaCl on the *trans* side (pH 8.0). Two to four successive curves are superimposed for each toxin sample; their slope becomes steeper with time because the number of channels inserted into the bilayer increases. All the curves of a family intercept the voltage axis at one point. Such voltage, at which no net current flows through the channel is called reversal voltage (V_{rev}). A negative value of V_{rev} indicates that the pore is cation selective; ideal cation selectivity under these conditions would give $V_{rev} = -52$ mV. PLM were exposed either to 6.5 μg/ml native toxin (curve *a*), or to 3.9 μg/ml PLP-modified toxin (curve *b*), or to 2.7 μg/ml EDC-modified toxin (curve *c*). In curve *b* the number of lysine residues modified per toxin monomer (estimated spectrophotometrically) was 3.4; in curve *c* the number of carboxyl groups modified per toxin monomer (derived by amino acid analysis) was nine. (*B*) Current-voltage curves obtained applying short square-shaped voltage pulses [37] to membranes containing many toxin channels are shown. The membrane was prepared in Buffer A (pH 8.0) and exposed either to 0.25 μg/ml native toxin (squares), or to 0.9 μg/ml PLP-modified toxin (circles). Each curve is the mean of two independent experiments scaled by dividing by the current flowing at −40 mV. Other conditions as in *A*. (*C*) Cartoon illustrating a distribution of the electrical charges inside the pore, before and after chemical modification, which accounts for its observed electrical properties. (*a*) native channel: carboxyl groups line the lumen of the *cis* entrance whereas both lysines and carboxyl groups line the *trans* entrance. The overall excess of negative charges accounts for the cation selectivity of the pore (attracting cations and repelling anions from inside the channel). The uneven distribution of the charges explains the nonlinearity of the *I-V* curve. In fact, because of the accumulation of negative charges near the *cis* entrance, the cation current flowing at negative voltages (i.e., from the *cis* side, which is grounded, to the *trans* side) is larger than that flowing in the opposite direction when positive voltages of the same value are applied. (*b*) PLP-modified channel: the positive charge of the lysines located at the *trans* entrance are changed to negative. As a consequence, both the cation selectivity and the conductance of the pore increase (more cations and less anions are attracted inside the channel) but the nonlinearity of the *I-V* curve disappears because the charges are now evenly distributed. (*c*) EDC-modified channel: the negative charge of some carboxyl groups is neutralized so that the net charge becomes zero. As a consequence the cation selectivity is lost and the conductance of the pore reduced to a minimum (no attractive effect).

number of events observed with their conductance, for native and chemically-modified toxin (Fig. 6*B*), shows that PLP modification increased the pore conductance whereas EDC-modification strongly decreased it. This indicated a positive correlation between the pore conductance and the amount of negative charge on the toxin.

The ion selectivity of the channel was then investigated by measuring the reversal voltage (i.e., the voltage at which the net flowing current is zero) for membranes with a large number of pores, separating a tenfold concentration gradient of NaCl (Fig. 7*A*). This voltage, called V_{rev}, was large and negative in the case of native toxin indicating that the pore was cation selective. PLP modification of lysine residues increased the cation selectivity of the pore even more, whereas EDC modification of carboxyl groups completely abrogated it. Again, this indicated a positive correlation between cation selectivity of the pore and amount of negative charge on the toxin.

The prominent role of charged groups in determining the pore properties was confirmed by the analysis of its current-voltage (*I-V*) characteristics (Fig. 7*B*). The *I-V* curve of native EqT-II pores was nonlinear, in fact the current flowing at negative voltages was larger than that flowing at positive voltages of the same value. In general, this implies that

Table 2. Effects of chemical modification on the electrical properties of EqT-II pores

Toxin sample	Conductance[a] (pS)	V_{rev}[b] (mV)	P(Na)/P(Cl)[c]	I(−)/I(+)[d]
Native	225 ± 10 (52)	−38 ± 2	9 ± 1	1.6
PLP-modified	316 ± 33 (23)	−49.5 ± 1.5	44 ± 15	1.0
EDC-modified	30 ± 5 (27)	0.3 ± 0.2	0.98 ± 0.01	—

[a] Single channel conductance ± SEM, at +40 mV in a PLM. The number of events used is given in parentheses.
[b] Reversal voltage derived as shown in Fig. 7 using a 10-fold NaCl gradient. Errors are standard deviations of two to four independent experiments run on different PLM membranes.
[c] Sodium to chloride permeability ratio calculated from V_{rev} according to the Nernst-Planck equation [19].
[d] Ratio between the current flowing at −120 mV and that at +120 mV (in absolute value) derived as shown in Fig. 7 for PLM membranes.

the potential profile of the pore (generated by its own fixed charges) is asymmetrical along the ion pathway [30, 48]. In this case PLP modification made the *I-V* curve linear. This finding suggests the presence of some lysine residues at well-defined positions along the ion pathway which can affect the potential profile of the pore.

The electrical properties of pores formed by native and modified toxins are summarized in Table 2. There we report the pore conductance, the reversal voltage V_{rev}, the ratio between sodium and chloride permeability derived through the Nernst-Planck equation [19], and, as a measure of the nonlinearity of the *I-V* curve, the ratio between the current flowing at +120 mV and that at −120 mV.

Discussion

All the evidence presented in this paper indicates that sea anemone cytolysin EqT-II increases the permeability of native, as well as model membranes, by opening discrete ionic channels. An estimate of the size of the pore which is formed on the erythrocyte membrane was obtained by measuring the transit time of sugars of different size and applying the Renkin equation [45], a method already successful with a number of porins [39, 40, 57] and of exogenously induced ion pathways in red blood cells [16]. We received a radius of 1.1 ± 0.1 nm. Since the assumptions necessary for the application of the Renkin equation, i.e., a perfectly cylindrical channel and a spherical diffusing molecule, are probably far from the real geometry of our system, this value has to be regarded as merely indicative. However, it is in reasonable agreement with the unit conductance of the pore measured in PLM (about 225 pS, *see* Table 2), which provides a radius of 0.9 nm (assuming a cylindrical cation-selective channel of 7-nm length).

Because the toxin was active against model membranes comprised of pure lipids, we believe that a receptor is not absolutely required for its action. It appears that sphingomyelin may act as a low-affinity receptor since it facilitates pore formation in model membranes (Fig. 3*C*) and it competes against hemolysis [52]. A similar sphingomyelin-dependent binding and insertion was observed with a related toxin from *Stichodactyla heliantus* [10] using lipid monolayers. However, HRBC lysed at EqT-II concentrations at which even the most sensitive vesicles remained unaffected, leaving open the hypothesis that a receptor other than sphingomyelin may exist on some cells.

The results indicate that toxin channels are probably oligomeric. We did not observe a single size for the oligomer but rather various coexisting sizes up to the heptamer at least (Fig. 5). This might still implicate that the size of the aggregate is fixed and large, and that the reactivity to the cross-linker is very low, as observed for example with the hexameric channel formed by the membrane protein synaptophysin [22, 51] and the pentameric postsynaptic glycine-receptor channel [27]. Alternatively, it is also possible that the pore does not have a fixed structure but rather fluctuates in size by occasional addition of single monomers which come into contact by lateral diffusion into the plane of the membrane (as for the alamethicin channel [6, 28, 46]). This hypothesis is consistent with the observation of more than one conductive state for each single channel (Fig. 6*A*).

However, if we compare the relative probability of occurrence of each oligomeric state, derived by the optical density of the corresponding band, with

the theoretical predictions of a purely collisional model (as described in ref. [9]), we find a poor fit (Fig. 5). In fact, the model predicts more dimers and less of all the other oligomers than we found experimentally. Actually, a much better fit is found when a model for a preexisting tetramer is used (also derived from ref. [9]). In view of these results and those shown in Fig. 4*C*, i.e., a power dependence of about three in the dose response of the rate of SUV permeabilization, we suggest that EqT-II increases membrane permeability by forming oligomeric channels comprising an average of three to four copies of the toxin monomer, although occasionally larger aggregates may form. This is consistent with previous results obtained by others with the parent *S. heliantus* cytolysin for which a power dependence of four was observed in the dose dependence of the rate of pore formation in BLM [55]. A similar situation was also observed with cytolysin A III from the nemertine *Cerebratulus lacteus* [31].

Based on the electrical properties of pores formed by native EqT-II and modified toxins in PLM we can propose a model of the distribution of the electrical charges inside the channel lumen which accounts for the observed features (shown in Fig. 7*C*). This model is based on the following simple considerations: (i) being cation selective (Table 2) the EqT-II pore is probably lined by a negative charge which attracts cations and repels anions, thus increasing the rate of cation transport; (ii) because lysine-charge reversal (more negative charge) increases the cation selectivity, whereas carboxyl-groups neutralization (less negative charge) decreases the cation selectivity, both lysines and carboxyl groups conceivably line the lumen of the channel, leaving altogether an excess of negative residues, (iii) since the conductance of the channel is increased by lysine-charge reversal (more negative charge) and decreased by carboxyl-groups neutralization (less negative charge) the assumption of the preceding point ii is reinforced; (iv) finally, because the *I-V* curve of the native channel is nonlinear, the potential profile of the pore (generated by its charges) is asymmetrical along the ion pathway, i.e., the fixed charges are distributed unevenly. In particular, because the cation current flowing at negative voltages (i.e., from the *cis* to the *trans* entrance of the pore) is larger than that flowing at positive voltages of the same value, the most general electrodiffusional models [30, 48] suggest that more negative charges are located near the *cis* entrance of the channel. Furthermore, because PLP-modified toxin has a linear current-voltage curve, we conclude that the modified lysine residues are located near the *trans* entrance of the pore. A similar asymmetrical distribution of charged residues of different signs has been demonstrated previously for other aqueous channels, e.g., *S. aureus* α-toxin [7] and porins [3, 47].

We want to thank Ms. Susan Struthers for kindly correcting the manuscript. This work was supported financially by the Italian Ministero dell'Università e della Ricerca Scientifica e Tecnologica, by Consiglio Nazionale delle Richerche and by a grant from the University of Trento in partial fulfillment of a protocol of collaboration between the Universities of Trento and Ljubljana. G.B. was the recipient of a fellowship from the Fondazione Trentina per la Ricerca sui Tumori.

References

1. Batista, U., Maček, P., Sedmak, B. 1990. The cytotoxic and cytolytic activity of equinatoxin II from the sea anemone *Actinia equina*. *Cell Biol. Int. Rep.* **14:**1013–1024
2. Belmonte, G., Cescatti, L., Ferrari, B., Nicolussi, T., Ropele, M., Menestrina, G. 1987. Pore formation by *Staphylococcus aureus* alpha-toxin in lipid bilayers: dependence upon temperature and toxin concentration. *Eur. Biophys. J.* **14:**349–358
3. Benz, R. 1988. Structure and function of porins from gram-negative bacteria. *Annu. Rev. Microbiol.* **42:**359–393
4. Bernheimer, A. W., Rudy, B. 1986. Interactions between membranes and cytolytic peptides. *Biochim. Biophys. Acta* **864:**123–141
5. Bhakdi, S., Muhly, M., Fussle, R. 1984. Correlation between toxin binding and hemolytic activity in membrane damage by Staphylococcal alpha-toxin. *Infect. Immun.* **46:**318–323
6. Boheim, G., Kolb, H. A. 1978. Analysis of the multi-pore system of alamethicin in a lipid membrane. I. Voltage-jump current-relaxation measurements. *J. Membrane Biol.* **39:** 99–150
7. Cescatti, L., Pederzolli, C., Menestrina, G. 1991. Modification of lysine residues of *S. aureus* α-toxin: effects on its channel forming properties. *J. Membrane Biol.* **119:**53–64
8. Davies, G. E., Stark, G. R. 1970. Use of dimethyl suberimidate, a cross-linking reagent, in studying the subunit of oligomeric proteins. *Proc. Natl. Acad. Sci. USA* **66:**651–656
9. Downer, N. W. 1985. Cross-linking of dark-adapted frog photoreceptor disk membranes. Evidence for monomeric rhodopsin. *Biophys. J.* **47:**285–293
10. Doyle, J. W., Kem, W. R., Villalonga, R. A. 1989. Interfacial activity of an ion channel-generating cytolysin from the sea anemone *Stichodactyla heliantus*. *Toxicon* **27:**465–471
11. Fleer, E. A., Verheij, H. M., de Haas, G. H. 1981. Modification of carboxylate groups in bovine pancreatic phospholipase A_2. Identification of aspartate 49 as Ca^{++} binding ligand. *Eur. J. Biochem.* **113:**283–288
12. Forti, S., Menestrina, G. 1989. Staphylococcal alpha-toxin increases the permeability of lipid vesicles by a cholesterol and pH dependent assembly of oligomeric channels. *Eur. J. Biochem.* **181:**767–773
13. Freer, J.H., Arbuthnott, J. P., Bilcliffe, B. 1973. Effects of staphylococcal alpha-toxin on the structure of erythrocytes membranes. *J. Gen. Microbiol.* **75:**321–332
14. Füssle, R., Bhakdi, S., Sziegoleit, A., Tranum-Jensen, J., Kranz, T., Wellensiek, H. J. 1981. On the mechanism of membrane damage by *Staphylococcus aureus* alpha-toxin. *J. Cell Biol.* **91:**83–94
15. Garland, W.J., Buckley, J.T. 1988. The cytolytic toxin aero-

lysin must aggregate to disrupt erythrocytes, and aggregation is stimulated by human glycophorin. *Infect. Immun.* **56:** 1249–1253
16. Ginsberg, H., Stein, W.D. 1987. Biophysical analysis of novel transport pathways induced in red blood cell membranes. *J. Membrane Biol.* **96:**1–10
17. Green, M.J., Buckley, J.T. 1990. Site-directed mutagenesis of the hole-forming toxin aerolysin: studies on the roles of histidines in receptor binding and oligomerization of the monomer. *Biochemistry* **29:**2177–2180
18. Harvey, H.L. 1990. Cytolytic toxins. *In:* Handbook of Toxinology. W.T. Shier, D. Mebs, editors, pp. 1–66. Marcel Dekker, New York
19. Hille, B. 1984. Ionic Channels of Excitable Membranes. Sinauer, Sunderland, MA
20. Ho, C.L., Ko, J.L., Lue, H.M., Lee, C.Y., Ferlan, I. 1987. Effect of equinatoxin on the guinea-pig atrium. *Toxicon* **25:**659–664
21. Hollecker, M., Creighton, T.E. 1980. Counting integral numbers of amino groups per polypeptide chain. *FEBS Lett.* **119:**187–189
22. Johnston, P.A., Südhof, T.C. 1990. The multisubunit structure of synaptophysin. Relationship between disulfide bonding and homo-oligomerization. *J. Biol. Chem.* **265:**8869–8873
23. Kem, W.R. 1988. Sea anemone toxin: Structure and action. *In:* The Biology of Nematocysts. D.A. Hessinger, H.M. Lenhoff, editors. pp. 375–405. Academic, San Diego
24. Kuga, S. 1981. Pore size distribution analysis of gel substances by size exclusion chromatography. *J. Chromatography* **206:**449–461
25. Laemmli, U.K. 1970. Cleavage of structural proteins during the assembly of the head of bacteriophage T4. *Nature* **227:**680–685
26. Lafranconi, W.M., Ferlan, I., Russell, F.E., Huxtable, R.J. 1984. The action of equinatoxin, a peptide from the venom of the sea anemone, *Actinia equina*, on isolated lung. *Toxicon* **22:**347–352
27. Langosch, D., Thomas, L., Betz, H. 1988. Conserved quaternary structure of ligand-gated ion channels: the postsynaptic glycine receptor is a pentamer. *Proc. Natl. Acad. Sci. USA* **85:**7394–7398
28. Latorre, R., Alvarez, O. 1981. Voltage dependent channels in planar lipid bilayer membranes. *Physiol. Rev.* **61:**77–150
29. Lee, C.Y. 1989. Cardiovascular effects of equinatoxin, a basic protein from the sea anemone, *Actinia equina*. *In:* Biosignalling in Cardiac and Vascular Systems. M. Fujiwara, S. Narumiya, S. Miwa, editors. pp. 380–384. Pergamon, Oxford
30. Lindemann, B. 1982. Dependence of ion flow through channels on the density of fixed charges at the channel opening; Voltage control of inverse titration curve. *Biophys. J.* **39:**15–22
31. Liu, J., Blumenthal, K.M. 1988. Functional interaction between *Cerebratulus lacteus* cytolysin A-III and phospholipase A_2. Implication for the mechanism of cytolysis. *J. Biol. Chem.* **263:**6619–6624
32. Maček P., Lebez, D. 1981. Kinetics of hemolysis induced by equinatoxin, a cytolitic toxin from the sea anemone *Actinia equina*. Effect of some ions and pH. *Toxicon* **19:**233–240
33. Maček, P., Lebez, D. 1988. Isolation and characterization of three lethal and hemolytic toxins from the sea anemone *Actinia equina* L. *Toxicon* **26:**441–451
34. Menestrina, G. 1988. *Escherichia coli* hemolysin permeabilizes small unilamellar vesicles loaded with calcein by a single hit mechanism. *FEBS Lett.* **232:**217–220
35. Menestrina, G. 1991. Electrophysiological methods for the study of toxin-membrane interaction. *In:* Sourcebook of Bacterial Protein Toxins. J.E. Alouf, J.H. Freer, editors. pp. 215–241. Academic, London.
36. Menestrina, G. 1991. Pore-forming cytolysins studied with planar lipid membranes. *Period Biol.* 93:201–206.
37. Menestrina, G., Antolini, R. 1982. The dependence of the conductance of the hemocyanin channel on applied potential and ionic concentration with mono and divalent cations. *Biochim. Biophys. Acta* **688:**673–684
38. Michaels, D.W. 1979. Membrane damage by a toxin from the sea anemone *Stoichactis helianthus*. 1. Formation of transmembrane channels in lipid bilayers. *Biochim. Biophys. Acta* **555:**67–78
39. Nikaido, H., Rosenberg, E.Y. 1983. Porin channels in *Escherichia coli:* studies with liposomes reconstituted from purified proteins. *J Bacteriol.* **153:**241–252
40. Nikaido, H., Rosenberg, Y. 1981. Effect of solute size on diffusion rates through the transmembrane pores of outer membrane of *Escherichia coli*. *J. Gen. Physiol.* **77:**121–135.
41. Nishigori, H., Toft, D. 1979. Modification of avian progesteron receptor by pyridoxal-5′-phosphate. *J. Biol. Chem.* **254:**9155–9161
42. Norton, R.S. 1991. Structure and structure-function relationship of sea anemone proteins that interact with the sodium channel. *Toxicon* **29:**1051–1084
43. Peach, C., Tolbert, N.E. 1978. Active site studies of ribulose-1,5-bisphosphate carboxylase/oxygenase with pyridoxal-5′-phosphate. *J. Biol. Chem.* **253:**7864–7873
44. Pederzolli, C., Cescatti, L., Menestrina, G. 1991. Chemical modification of *Staphylococcus aureus* α-toxin by diethylpyrocarbonate: role of histidines in its membrane damaging properties. *J. Membrane Biol.* **119:**41–52
45. Renkin, E.M. 1954. Filtration, diffusion, and molecular sieving through porous cellulose membranes. *J. Gen. Physiol.* **38:**225–243
46. Rizzo, V., Stankowski, S., Schwarz, G. 1987. Alamethicin incorporation in lipid bilayers: a thermodynamic study. *Biochemistry* **26:**2751–2759
47. Rosenbusch, J.P. 1990. Structural and functional properties of porin channels in *E. coli* outer membranes. *Experientia* **46:**167–173
48. Schultz, S.G. 1980. Basic principles of membrane transport. Cambridge University, New York
49. Schultz, S.G., Solomon, A.K. 1961. Determination of the effective hydrodynamic radii of small molecules by viscometry. *J. Gen. Physiol.* **44:**1189–1199
50. Teng, C.M., Lee,L.G., Lee, C.Y., Ferlan, I. 1988. Platelet aggregation induced by equinatoxin. *Thromb. Res.* **52:**401–411
51. Thomas, L., Hartung, K., Langosch, D., Rehm, H., Bamberg, E., Franke, W.W., Betz, H. 1988. Identification of synaptophysin as a hexameric channel protein of the synaptic vesicle membrane. *Science* **242:**1050–1052
52. Turk, T., Maček, P. 1986. Effect of different membrane lipids on the hemolytic activity of equinatoxin II from *Actinia equina*. *Period. Biol.* **88:**216–217
53. Turk, T., Maček, P. 1992. The role of lysine, histidine and carboxyl residues in biological activity of equinatoxin II, a

pore forming polypeptide from the sea anemone *Actinia equina* L. *Biochim. Biophys. Acta* **1119:**5–10

54. Turk, T., Maček, P., Gubenšek, F. 1989. Chemical modification of equinatoxin II, a lethal and cytolytic toxin from the sea anemone *Actinia equina*. *Toxicon* **27:**357–384
55. Varanda, A., Finkelstein, A. 1980. Ion and non electrolyte permeability properties of channels formed in planar lipid bilayer membranes by the cytolytic toxin from the sea anemone, *Stoichactis helianthus*. *J. Membrane Biol.* **55:** 203–211.
56. Weiner, R.N., Schneider, E., Haest, C.W.M., Deuticke, B., Benz, R., Frimmer, M. 1985. Properties of the leak permeability induced by a cytotoxic protein of *Pseudomonas aeruginosa* (PACT) in rat erythrocytes and black lipid membranes. *Biochim. Biophys. Acta* **820:**173–182
57. Yoshimura, F., Zalman, L.S., Nikaido, H. 1983. Purification and properties of *Psuedomonas aeruginosa* porin. *J. Biol. Chem.* **258:**2308–2314
58. Zorec, R., Tester, M., Maček, P., Mason, W.T. 1990. Cytotoxicity of equinatoxin II from the sea anemone *Actinia equina* involves ion channel formation and an increase in intracellular calcium activity. *J. Membrane Biol.* **118:**243–249

Received 13 December 1991; revised 1 June 1992